

# Measuring light-by-light scattering at the LHC and FCC\*

DAVID D'ENTERRIA

CERN, EP Department, 1211 Geneva, Switzerland

GUSTAVO G. DA SILVEIRA

Instituto de Física e Matemática, Univ. Fed. de Pelotas, Caixa Postal 354,  
CEP 96010-090, Pelotas, RS, Brazil

Elastic light-by-light scattering,  $\gamma\gamma \rightarrow \gamma\gamma$ , can be measured in electromagnetic interactions of lead (Pb) ions at the Large Hadron Collider (LHC) and Future Circular Collider (FCC), using the large (quasi)real photon fluxes available in ultraperipheral collisions. The  $\gamma\gamma \rightarrow \gamma\gamma$  cross sections for diphoton masses  $m_{\gamma\gamma} > 5$  GeV in p-p, p-Pb, and Pb-Pb collisions at LHC ( $\sqrt{s_{NN}} = 5.5, 8.8, 14$  TeV) and FCC ( $\sqrt{s_{NN}} = 39, 63, 100$  TeV) center-of-mass energies are presented. The measurement has controllable backgrounds in Pb-Pb collisions, and one expects about 70 and 2 500 signal events per year at the LHC and FCC respectively, after typical detector acceptance and reconstruction efficiency selections.

PACS numbers: 12.20.-m, 13.40.-f, 14.70.-e, 25.20.Lj

## 1. Introduction

The elastic scattering of two photons in vacuum,  $\gamma\gamma \rightarrow \gamma\gamma$ , is a pure quantum mechanics process that proceeds at leading order (LO) in the fine structure constant,  $\mathcal{O}(\alpha^4)$ , via virtual box diagrams containing charged particles. In the standard model (SM), the box diagram of Fig. 1 involves charged fermions (leptons and quarks) and boson ( $W^\pm$ ) loops. Despite its simplicity, light-by-light (LbyL) scattering remains still unobserved today because of its tiny cross section  $\sigma_{\gamma\gamma} \propto \mathcal{O}(\alpha^4) \approx 3 \cdot 10^{-9}$ , although the electron loop contribution has been precisely, yet indirectly, tested in the anomalous electron and muon magnetic moments measurements. Out of the two closely-related processes –photon scattering in the Coulomb field of a nucleus (Delbrück scattering) and photon-splitting in a strong magnetic field (vacuum birefringence)– only the former has been experimentally observed [1]. Apart from the intrinsic importance of its direct observation in the laboratory,  $\gamma\gamma$  scattering provides a particularly neat channel to study anomalous gauge couplings [2], and search for physics beyond the SM (BSM) through new heavy charged particles contributing to the virtual loop in Fig. 1 –in particular at high diphoton invariant masses– such as *e.g.* SUSY particles [3]. LbyL scattering has also been proposed as a means to search for monopoles [4], axions [5], unparticles [6], low-scale gravity effects [7], and non-commutative interactions [8].

Several approaches have been proposed to experimentally detect  $\gamma\gamma \rightarrow \gamma\gamma$  using *e.g.* Compton-backscattered photons against laser photons [9], collisions of

---

\* Proceedings EDS'15 Blois Conference, Corsica, June 2015

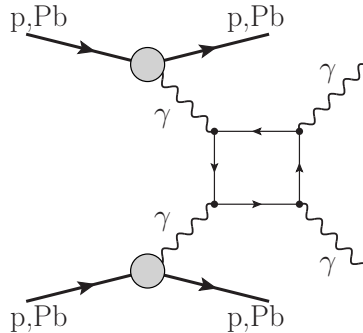


Fig. 1. Diagram of elastic  $\gamma\gamma \rightarrow \gamma\gamma$  collisions in ultraperipheral proton and/or ion interactions. The initial-state photons are emitted coherently by the protons and/or nuclei, which survive the electromagnetic interaction.

photons from microwave waveguides/cavities [10] or high-power lasers [11], as well as at photon colliders [2] where energetic  $\gamma$  beams can be obtained by Compton-backscattering laser-light off  $e^+e^-$  beams. In [12] we demonstrated that one can detect elastic  $\gamma\gamma$  scattering using the large (quasi)real photon fluxes of the protons and ions accelerated at TeV energies at the CERN Large Hadron Collider (LHC). In this work, we summarize the results of [12] and extend the study for the energies of the Future Circular Collider (FCC), a new facility proposed for BSM searches in a new 80–100 km tunnel to be constructed at CERN [13].

## 2. Theoretical setup

All charges accelerated at high energies generate electromagnetic fields which, in the equivalent photon approximation (EPA) [14], can be considered as  $\gamma$  beams of virtuality  $-Q^2 < 1/R^2$ , where  $R$  is the radius of the charge, *i.e.*  $Q^2 \approx 0.08 \text{ GeV}^2$  for protons ( $R \approx 0.7 \text{ fm}$ ), and  $Q^2 < 4 \cdot 10^{-3} \text{ GeV}^2$  for nuclei ( $R_A \approx 1.2 A^{1/3} \text{ fm}$ , for mass number  $A > 16$ ). The photon spectra have a typical  $E_\gamma^{-1}$  power-law fall-off up to energies of the order of  $\omega_{\text{max}} \approx \gamma/R$ , where  $\gamma$  is the Lorentz relativistic factor of the proton or ion. Although the  $\gamma$  spectrum is harder for smaller charges –which favours proton over nuclear beams in the production of heavy diphoton systems– each photon flux scales with the squared charge of the beam,  $Z^2$ , and thus  $\gamma\gamma$  luminosities are extremely enhanced, up to  $Z^4 = 5 \cdot 10^7$  in the case of Pb-Pb, for ion beams. Table 1 summarizes the relevant parameters for ultraperipheral p-p, p-Pb, and Pb-Pb collisions at the LHC and FCC. Two-photon center-of-mass (c.m.) energies at the FCC will reach for the first time the multi-TeV range.

Photon-photon collisions in “ultraperipheral” collisions (UPCs) of proton [15] and lead (Pb) beams [16] have been experimentally measured at the LHC [17, 18, 19]. The UPC final-state signature in this work is the exclusive production of two photons,  $AB \xrightarrow{\gamma\gamma} A\gamma\gamma B$ , with the diphoton final-state measured in the central detector, and the hadrons  $A, B = p, \text{Pb}$  surviving the electromagnetic interaction scattered at very low angles with respect to the beam. The very same final-state can be mediated by the strong interaction through a quark-loop in the exchange of two gluons in a colour-singlet state,  $AB \xrightarrow{gg} A\gamma\gamma B$  [20]. Such “central exclusive production” (CEP), observed in  $p\bar{p}$  at Tevatron [21] and searched for at the

Table 1. Characteristics of  $\gamma\gamma \rightarrow \gamma\gamma$  measurements in AB collisions at LHC and FCC: (i) nucleon-nucleon c.m. energy,  $\sqrt{s_{\text{NN}}}$ , (ii) integrated luminosity  $\mathcal{L}_{\text{AB}} \cdot \Delta t$  ( $\mathcal{L}_{\text{AB}}$  are beam luminosities –for low pileup in the p-p case– and a “year” is  $\Delta t = 10^7$  s for p-p, and  $10^6$  s in the ion mode), (iii) beam Lorentz factor,  $\gamma$ , (iv) maximum photon energy in the c.m. frame,  $\omega_{\text{max}}$ , (v) maximum photon-photon c.m. energy,  $\sqrt{s_{\gamma\gamma}^{\text{max}}}$ , (vi) cross section for  $\gamma\gamma$  masses above 5 GeV, and (vii) expected number of counts/year after selection cuts.

System	$\sqrt{s_{\text{NN}}}$ (TeV)	$\mathcal{L}_{\text{AB}} \cdot \Delta t$ (per year)	$\gamma$ ( $\times 10^3$ )	$\omega_{\text{max}}$ (TeV)	$\sqrt{s_{\gamma\gamma}^{\text{max}}}$ (TeV)	$\sigma_{\gamma\gamma \rightarrow \gamma\gamma}^{\text{excl}}$ [ $m_{\gamma\gamma} > 5$ GeV]	$N_{\gamma\gamma}^{\text{cuts}}$
p-p	14	1 fb $^{-1}$	7.5	2.45	4.5	105 $\pm$ 10 fb	12
p-Pb	8.8	200 nb $^{-1}$	4.7	0.13	0.26	260 $\pm$ 26 pb	6
Pb-Pb	5.5	1 nb $^{-1}$	2.9	0.80	0.16	370 $\pm$ 70 nb	70
p-p	100	1 fb $^{-1}$	53.	17.6	35.2	240 $\pm$ 24 fb	50
p-Pb	63	1 pb $^{-1}$	33.5	0.95	1.9	780 $\pm$ 78 pb	150
Pb-Pb	39	5 nb $^{-1}$	21.	0.60	1.2	1.85 $\pm$ 0.37 $\mu$ b	2 500

LHC [17], constitutes an important background for the  $\gamma\gamma \rightarrow \gamma\gamma$  measurement in p-p but not Pb-Pb collisions as discussed later. In the EPA, the elastic  $\gamma\gamma$  production cross section in UPCs of hadrons A and B factorizes into the product of the elementary  $\gamma\gamma \rightarrow \gamma\gamma$  cross section at  $\sqrt{s_{\gamma\gamma}}$ , convolved with the photon fluxes  $f_{\gamma/A,B}(\omega)$  of the two colliding beams:

$$\sigma_{\gamma\gamma \rightarrow \gamma\gamma}^{\text{excl}} = \sigma(\text{AB} \xrightarrow{\gamma\gamma} \text{A}\gamma\gamma\text{B}) = \int d\omega_1 d\omega_2 \frac{f_{\gamma/A}(\omega_1)}{\omega_1} \frac{f_{\gamma/B}(\omega_2)}{\omega_2} \sigma_{\gamma\gamma \rightarrow \gamma\gamma}(\sqrt{s_{\gamma\gamma}}), \quad (1)$$

where  $\omega_1$  and  $\omega_2$  are the energies of the photons emitted by hadrons A and B. We use the proton  $f_{\gamma/p}(\omega)$  spectrum derived from its elastic form factor [22] and, the impact-parameter dependent expression for the ion  $f_{\gamma/A}(\omega)$  spectrum [23], including a correction equivalent to ensuring that all collisions are purely exclusive, *i.e.* without hadronic overlap and breakup of the colliding beams [24]. The MADGRAPH v.5 Monte Carlo (MC) [25] framework is used to convolve the  $\gamma$  fluxes as done in [26], with the LO expression for the  $\sigma_{\gamma\gamma \rightarrow \gamma\gamma}$  cross section [27] including all quark and lepton loops. We omit the  $W^\pm$  contributions which are only important at  $m_{\gamma\gamma} \gtrsim 200$  GeV. Inclusion of next-to-leading-order QCD and QED corrections increases  $\sigma_{\gamma\gamma \rightarrow \gamma\gamma}$  by a few percent [27], which are nonetheless “compensated” by the  $\hat{S}^2 = 0.9\text{--}1.0$  gap survival factor –encoding the probability to produce the  $\gamma\gamma$  system without any other hadronic activity from soft rescatterings between the colliding hadrons [20]– that reduces the exclusive yields by about the same amount. Propagated uncertainties to the final cross sections are of order  $\pm 10\%$  ( $\pm 20\%$ ) for p-p and p-Pb (Pb-Pb) collisions, covering different form-factors parametrizations and the convolution of the nuclear photon fluxes.

Our calculations require diphoton masses in the continuum above  $m_{\gamma\gamma} = 5$  GeV, avoiding the region of two-photon decays from CEP hadronic resonances (*e.g.*  $\chi_{c0,c2} \rightarrow \gamma\gamma$  at masses 3.4–3.9 GeV), and where one can easily define an experimental trigger based on a few GeV deposit in the calorimeters. Also, for lower diphoton masses, the  $\gamma\gamma$  cross section has larger theoretical uncertainties as the hadronic LbyL contributions are computed less reliably by the quark boxes [27].

### 3. Signal cross sections

Using the theoretical setup described, we obtain the values of  $\sigma_{\gamma\gamma}^{\text{excl}}$  listed in Table 1 and plotted as a function of c.m. energies in the range  $\sqrt{s_{\text{NN}}} = 1\text{--}100$  TeV in Fig. 2. The cross sections are in the hundreds of fb/pb/nb for p-p, p-Pb, and Pb-Pb (and even, remarkably, at the  $\mu\text{b}$  level for the latter at the FCC), clearly showing the importance of the  $Z^4$  photon-flux enhancement for ions compared to protons. The increase in cross sections from LHC to FCC is of  $\mathcal{O}(2\text{--}5)$ . The

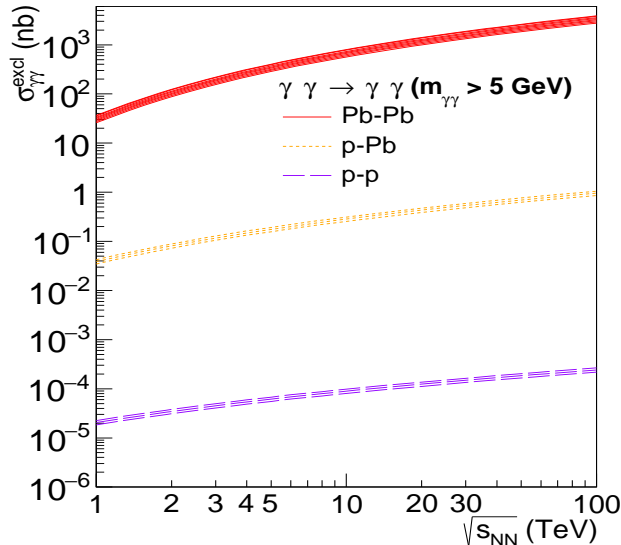


Fig. 2. Cross sections for  $\gamma\gamma \rightarrow \gamma\gamma$ , with pair masses above 5 GeV, in ultraperipheral Pb-Pb (top curve), p-Pb (middle) and p-p (bottom) collisions as a function of c.m. energy.

detectable number of  $\gamma\gamma \rightarrow \gamma\gamma$  events at the LHC and FCC are estimated by considering nominal luminosities for each system, geometric detector acceptance, and reconstruction efficiencies. For the LHC (FCC) we consider photon detection capabilities with tracking and calorimetry over pseudorapidities  $|\eta| < 2.5$  (5.0), plus forward detectors, up to at least  $|\eta| = 5$ , to select exclusive events requiring rapidity-gaps on both sides of the central diphoton system. The requirement to have both photons with  $p_{\text{T}}^{\gamma} > 2$  GeV within the  $|\eta|$  ranges considered, reduces the yields by  $\varepsilon_{\text{acc}} \approx 0.2$  (0.3) in p-p and p-Pb, and by  $\varepsilon_{\text{acc}} \approx 0.3$  (0.4) in Pb-Pb collisions at the LHC (FCC). The acceptance is larger in the Pb-Pb case because the EPA fluxes are softer and the  $\gamma\gamma$  system is produced at more central rapidities. We also consider offline  $\gamma$  reconstruction and identification efficiencies  $\varepsilon_{\text{rec,id}\gamma} \approx 0.8$  in the photon energy range of interest. The final combined signal efficiency is  $\varepsilon_{\text{pp,pPb}\rightarrow\gamma\gamma} = \varepsilon_{\text{trig}} \cdot \varepsilon_{\text{acc}} \cdot \varepsilon_{\text{rec,id}\gamma}^2 \approx 12\%$  (20%) for p-p and p-Pb, and  $\varepsilon_{\text{PbPb}\rightarrow\gamma\gamma} \approx 20\%$  (26%) for Pb-Pb, at the LHC (FCC). The number of events expected per year ( $\Delta t = 10^6$  s in the ion mode,  $10^7$  s for p-p) are obtained via  $N_{\gamma\gamma}^{\text{excl}} = \varepsilon_{\gamma\gamma} \cdot \sigma_{\gamma\gamma}^{\text{excl}} \cdot \mathcal{L}_{\text{AB}} \cdot \Delta t$  (Table 1). The nominal p-Pb and Pb-Pb luminosities are low enough to keep the number of simultaneous collisions well below one, and one can take their full integrated luminosity as usable for the exclusive measurement. In p-p, pileup is very high and we consider that only  $1 \text{ fb}^{-1}/\text{year}$  can be collected under conditions that preserve the rapidity gaps adjacent to the central  $\gamma\gamma$  system. Clearly, Pb-Pb provides the best signal counting rates, with statistical

uncertainties of order  $\sqrt{N_{\gamma\gamma}^{\text{excl}}} = \pm 12\%_{(\text{LHC})}, 2\%_{(\text{FCC})}$ , free of pileup complications.

#### 4. Backgrounds, and $\gamma\gamma \rightarrow \gamma\gamma$ significances

There are three potential backgrounds that share the same (or very similar) final-state signature as  $\gamma\gamma \rightarrow \gamma\gamma$ : (i) central-exclusive diphoton production<sup>1</sup>  $gg \rightarrow \gamma\gamma$ , (ii) QED  $\gamma\gamma \rightarrow e^+e^-$  events, with both  $e^\pm$  misidentified as photons, and (iii) diffractive Pomeron-induced (*IP*IP, or  $\gamma$ IP) processes with final-states containing two photons plus rapidity gaps. The latter diffractive and  $\gamma$ -induced final-states have larger  $p_T^{\gamma\gamma}$  and diphoton acoplanarities than  $\gamma\gamma \rightarrow \gamma\gamma$ , and can be efficiently removed. The CEP  $gg \rightarrow \gamma\gamma$  background, however, scales with the fourth power of the gluon density and is a large potential background. In the p-p case and for the range of  $m_{\gamma\gamma}$  considered here, we obtain a cross section after acceptance cuts of  $\sigma_{gg \rightarrow \gamma\gamma}^{\text{CEP}} = 20_{\times 1/3}^{\times 3}$  pb at the LHC with SUPERCHIC 1.41 [20], where the large uncertainties include the choice of the parton distribution function (PDF) and  $\hat{S}^2$  survival factor. Typical CEP photon pairs peak at  $p_T^{\gamma\gamma} \approx 0.5$  GeV and have moderate tails in their azimuthal acoplanarity  $\Delta\phi_{\gamma\gamma}$ , whereas photon-fusion systems are produced almost at rest. By imposing very tight cuts in the pair momentum,  $p_T^{\gamma\gamma} \lesssim 0.1$  GeV and acoplanarity  $\Delta\phi_{\gamma\gamma} - \pi \lesssim 0.04$ , the CEP  $\gamma\gamma$  can be reduced by a factor of about  $\times 90$  with minimum losses of the elastic  $\gamma\gamma$  signal. However, the resulting LbyL/CEP  $\approx 1/20$  ratio is still too large to make feasible the LbyL observation with proton beams. The situation is more advantageous for p-Pb, where the LbyL cross section is only about 6 times smaller than the CEP one, obtained scaling by  $A = 208$  the p-p cross section at 8.8 TeV ( $\sigma_{gg \rightarrow \gamma\gamma}^{\text{CEP}} = 16_{\times 1/3}^{\times 3}$  pb), multiplied by the square of the Pb gluon shadowing,  $R_g^{\text{Pb/p}} \approx 0.7$  according to the EPS09 nuclear PDF [29]. A final LbyL/CEP  $\approx 1$  ratio is reachable applying the aforementioned  $p_T^{\gamma\gamma}$  and  $\Delta\phi_{\gamma\gamma}$  cuts. Yet, given the low p-Pb rates expected at the LHC (Table 1), a 5- $\sigma$  observation of LbyL scattering requires an increase of the luminosity from its conservative nominal value [26].

In the Pb-Pb case, the situation is more favourable given that parton-mediated exclusive or diffractive cross sections (which scale as  $A^2$  compared to p-p) play a comparatively smaller role than in p-p thanks to the  $Z^4$ -enhancement of electromagnetic interactions. The Pb-Pb CEP cross section, as obtained by  $A^2$ -scaling the  $\sigma_{gg \rightarrow \gamma\gamma}^{\text{CEP}} = 13_{\times 0.4}^{\times 2.5}$  pb cross section in p-p at 5.5 TeV, multiplied by  $(R_g^{\text{Pb/p}})^4 \approx 0.25$ , is comparable to  $\sigma_{\gamma\gamma \rightarrow \gamma\gamma}^{\text{excl}}$ . Adding a simple  $p_T^{\gamma\gamma} < 0.2$  GeV condition, reduces the CEP background by  $\sim 95\%$  without removing any signal event, resulting in a final LbyL/CEP  $\approx 10$  ratio. Other electromagnetic processes in Pb-Pb are, however, similarly enhanced by the  $Z^4$  factor and can constitute a potential background if the final-state particles are misidentified as photons. The very large exclusive Pb-Pb  $\gamma\gamma \rightarrow e^+e^-$  QED cross section,  $\sigma_{\gamma\gamma \rightarrow e^+e^-}^{\text{QED}}[m_{e^+e^-} > 5 \text{ GeV}] = 5.4$  mb according to STARLIGHT [30], can be of concern if neither  $e^\pm$  track is reconstructed or if both  $e^\pm$  undergo hard bremsstrahlung. Requiring both  $e^\pm$  to fall within the central acceptance and be singly misidentified as photons with probability  $f_{e \rightarrow \gamma} \approx 0.5\%$ , results in a residual  $\gamma\gamma \rightarrow \gamma_{(e^+)}\gamma_{(e^-)}$  contamination of  $\sim 20\%$  of

<sup>1</sup> For CEP  $\pi^0\pi^0$  and  $\eta^{(\prime)}\eta^{(\prime)}$ , decaying into multi-photon final-states, their  $\gamma$  branching ratios, acceptance plus  $m_{\gamma\gamma}$  cuts results in a negligible final contribution compared to CEP  $\gamma\gamma$  [28].

the visible LbyL cross section. In Pb-Pb at FCC(39 TeV), the CEP cross section within  $|\eta| < 5$  is very large:  $\sigma_{gg \rightarrow \gamma\gamma}^{\text{CEP}}[m_{\gamma\gamma} > 5 \text{ GeV}] = 1.3 \text{ nb} \times 208^2 \times (R_g^{\text{Pb/p}})^4 \approx 14 \mu\text{b}$  (with a factor of  $\sim 3$  uncertainty) obtained with SUPERCHIC 2.02 [31] and the MMHT2014 PDFs [32], reduced to  $\sim 400 \text{ nb}$  after cuts. The QED cross section is  $\sigma_{\gamma\gamma \rightarrow e^+e^-}^{\text{QED}}[m_{e^+e^-} > 5 \text{ GeV}] = 26 \text{ mb}$ , reduced to  $\sim 120 \text{ nb}$  after applying the  $f_{e \rightarrow \gamma}^2$  factor and acceptance selection criteria. After cuts, both backgrounds are thereby smaller than the expected visible LbyL cross section of  $\sim 500 \text{ nb}$ .

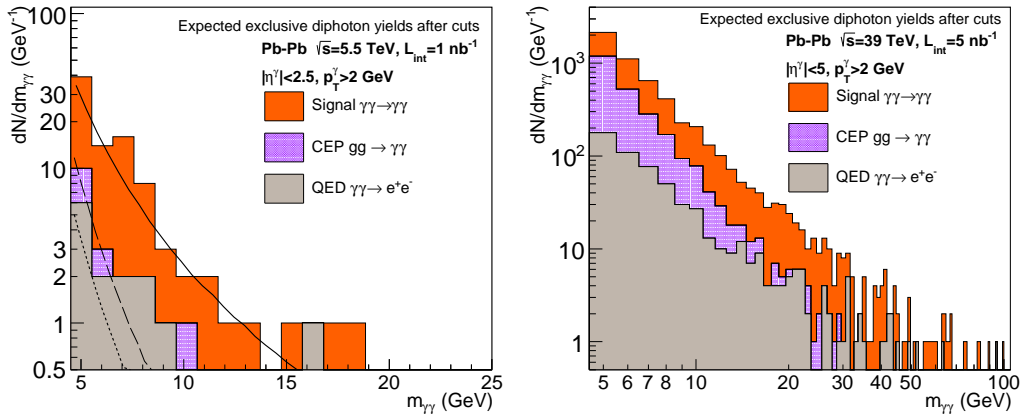


Fig. 3. Yields as a function of diphoton invariant mass for elastic  $\gamma\gamma$ , plus CEP- $\gamma\gamma$  and QED backgrounds, expected in Pb-Pb at LHC (left) and FCC (right) after analysis cuts.

Figure 3 shows the  $\gamma\gamma$  invariant mass distributions for signal and CEP and QED backgrounds after cuts in one Pb-Pb run at the LHC (left) [12] and FCC (right). At the LHC (FCC), we expect about  $N_{\gamma\gamma}^{\text{excl}} \approx 70$  (2 500) signal counts compared to  $\sim 6$  (2 000) and  $\sim 15$  (600) CEP and QED counts respectively, with FCC reaching much higher diphoton masses. The overall (profile likelihood) significances of the measurement are  $\mathcal{S} \approx 6$  at the LHC and  $\mathcal{S} \approx 35$  at FCC, considering 20% and 50% theoretical uncertainties on LbyL and CEP yields respectively (the QED  $e^+e^-$  background can be easily well measured beforehand).

## 5. Summary

We have shown that light-by-light scattering, a rare fundamental process that has escaped experimental observation so far, can be measured at the LHC and FCC exploiting the large quasireal photon fluxes in electromagnetic interactions of protons and ions accelerated at TeV energies. The  $\gamma\gamma \rightarrow \gamma\gamma$  cross sections for  $m_{\gamma\gamma} \geq 5 \text{ GeV}$  are in the hundreds fb,pb ranges for p-p,p-Pb, and reach the  $\mu\text{b}$  level for Pb-Pb at the FCC, clearly showing the importance of the  $Z^4$  enhancement of the photon fluxes in ion-ion collisions. The number of LbyL events expected in ATLAS and CMS have been estimated with realistic  $\gamma$  acceptance and efficiency cuts and integrated luminosities. In the p-p case, the dominant background due to exclusive gluon-induced  $\gamma\gamma$  production can be reduced imposing cuts on  $p_{\text{T}}^{\gamma\gamma}$  and pair acoplanarity, yet not to a level where the signal can be observed. The signal/background ratio is better in the p-Pb case but the small expected number of counts makes the LbyL measurement challenging without (reachable) luminosity increases. Observation of the process is possible in Pb-Pb

which provide  $N_{\gamma\gamma}^{\text{excl}} \approx 70$  elastic photon pairs per run after cuts at the LHC, with small backgrounds. The increase in  $\gamma\gamma \rightarrow \gamma\gamma$  yields from LHC to FCC is of  $\mathcal{O}(35)$  thanks to factors of  $\times 5$  larger cross sections and luminosities, and  $\times 2$  in the experimental acceptance. The measurement of elastic  $\gamma\gamma$  scattering at the LHC will be the first-ever observation of such fundamental quantum mechanical process in the lab. At the FCC, the higher-masses of the produced diphoton system may be sensitive to new-physics effects predicted in various SM extensions.

**Acknowledgments** - We thank Lucian Harland-Lang for valuable discussions and for independent cross-checks of some of our calculations.

## REFERENCES

- [1] G. Jarlskog *et al.*, Phys. Rev. D **8** (1973) 3813
- [2] S. J. Brodsky, and P. M. Zerwas, Nucl. Instrum. Meth. A **355** (1995) 19
- [3] G. J. Gounaris, P. I. Porfyriadis, and F. M. Renard, Eur. Phys. J. C **9** (1999) 673
- [4] I. F. Ginzburg and A. Schiller, Phys. Rev. D **57** (1998) 6599
- [5] D. Bernard, Nuovo Cim. A **110** (1997) 1339 [Nucl. Phys. Proc. Suppl. **72** (1999) 201]
- [6] T. Kikuchi, N. Okada and M. Takeuchi, Phys. Rev. D **77** (2008) 094012
- [7] K. -m. Cheung, Phys. Rev. D **61** (1999) 015005
- [8] J. L. Hewett, F. J. Petriello and T. G. Rizzo, Phys. Rev. D **64** (2001) 075012
- [9] K. O. Mikaelian, Phys. Lett. B **115** (1982) 267
- [10] G. Brodin, M. Marklund and L. Stenflo, Phys. Rev. Lett. **87** (2001) 171801
- [11] E. Lundstrom *et al.*, Phys. Rev. Lett. **96** (2006) 083602
- [12] D. d’Enterria, G. Silveira, Phys. Rev. Lett. **111** (2013) 080405; Erratum-ibid. (2016)
- [13] B. Benedikt *et al.*, IPAC-2015-TUPTY062.
- [14] C. von Weizsäcker *Z. Physik* **88** (1934) 612; E.J. Williams, Phys. Rev. **45** (1934) 729  
E. Fermi *Nuovo Cimento* **2** (1925) 143
- [15] D. d’Enterria, M.Klasen, K.Piotrkowski (eds.), Nucl. Phys. Proc. Suppl. B **179** (2008) 1
- [16] A. Baltz *et al.*, Phys. Rept. **458** (2008) 1
- [17] S. Chatrchyan *et al.* [CMS Collab.], JHEP **11** (2012) 080; JHEP **07** (2013) 116
- [18] E. Abbas *et al.* [ALICE Collab.], Eur. Phys. J. C **73** (2013) 2617
- [19] G. Aad *et al.* [ATLAS Collab.], Phys. Lett. B **749** (2015) 242
- [20] L. A. Harland-Lang *et al.*, Eur. Phys. J. C **69** (2010) 179
- [21] T. Aaltonen *et al.* [CDF Collab.], Phys. Rev. Lett. **108** (2012) 081801
- [22] V.M. Budnev, I.F. Ginzburg, G.V. Meledin, V.G. Serbo, Phys. Rept. **15** (1975) 181
- [23] C. A. Bertulani and G. Baur, Phys. Rept. **163** (1988) 299
- [24] R. N. Cahn and J. D. Jackson, Phys. Rev. D **42** (1990) 3690
- [25] J. Alwall *et al.*, JHEP **09** (2007) 028
- [26] D. d’Enterria and J.-Ph. Lansberg, Phys. Rev. D **81** (2010) 014004
- [27] Z. Bern *et al.*, JHEP **11** (2001) 031
- [28] L.A. Harland-Lang, V.A.Khoze, M.G.Ryskin and W.J.Stirling, EPJC **73** (2013) 2429
- [29] K.J. Eskola, H. Paukkunen and C.A. Salgado, JHEP **04** (2009) 065
- [30] J. Nystrand, Nucl. Phys. A **752** (2005) 470
- [31] L. A. Harland-Lang *et al.*, arXiv:1508.02718 [hep-ph]; <http://superchic.hepforge.org/>
- [32] L. A. Harland-Lang *et al.*, Eur. Phys. J. C **75** (2015) 5, 204